

Analytic multi-Baryonic solutions in the $SU(N)$ -Skyrme model at finite density

Sergio L. Cacciatori^{1,2} Fabrizio Canfora³ Marcela Lagos⁴ Federica Muscolino^{1,2} Aldo Vera⁴

¹*Università dell'Insubria, Dipartimento di Scienza ed Alta Tecnologia,
via Valleggio 11, 22100, Como, Italy*

²*INFN, via Celoria 16, 20133, Milano, Italy*

³*Centro de Estudios Científicos (CECS), Casilla 1469, Valdivia, Chile*

⁴*Instituto de Ciencias Físicas y Matemáticas, Universidad Austral de Chile,
Casilla 567, Valdivia, Chile*

E-mail: sergio.cacciatori@uninsubria.it, canfora@cecs.cl,
marcela.lagos@uach.cl, federica.muscolino@uninsubria.it,
aldo.vera@uach.cl

ABSTRACT: We construct explicit analytic solutions of the $SU(N)$ -Skyrme model (for generic N) suitable to describe different phases of nuclear pasta at finite volume in $(3 + 1)$ dimensions. The first type are crystals of Baryonic tubes (nuclear spaghetti) while the second type are smooth Baryonic layers (nuclear lasagna). Both, the ansatz for the spaghetti and the ansatz for the lasagna phases, reduce the complete set of Skyrme field equations to just one integrable equation for the profile within sectors of arbitrary high topological charge. We compute explicitly the total energy of both configurations in terms of the flavor number, the density and the Baryonic charge. Remarkably, our analytic results allow to compare explicitly the physical properties of nuclear spaghetti and lasagna phases. Our construction shows explicitly that, at lower densities, configurations with $N = 2$ light flavors are favored while, at higher densities, configurations with $N = 3$ are favored. Our construction also proves that in the high density regime (but still well within the range of validity of the Skyrme model) the lasagna configurations are favored while at low density the spaghetti configurations are favored. Moreover, the integrability property of the present configurations is not spoiled by the inclusion of the subleading corrections to the Skyrme model arising in the 't Hooft expansion. Finally, we briefly discuss the large N limit of our configurations.

Contents

1	Introduction	2
2	The theory	5
2.1	The $SU(N)$ -Skyrme model	5
2.2	General parameterization	6
3	Nuclear spaghetti phase	7
3.1	The ansatz	7
3.2	Solving the system analytically	8
3.3	A constraint from stability	9
3.4	Boundary conditions and Baryonic charge	10
3.5	Characterizing the $SU(N)$ nuclear spaghetti phase	11
4	Nuclear spaghetti versus nuclear lasagna	13
4.1	Review of the $SU(N)$ nuclear lasagna phase	13
4.2	Comparing nuclear spaghetti and lasagna at finite Baryon density	17
4.3	A comment on the large N limit	19
4.4	Subleading corrections	20
4.5	Isospin chemical potential	22
5	Conclusions and perspectives	23

1 Introduction

One of the most fascinating phenomena appearing when a large amount of Baryon charge is present within a finite volume (which has been confirmed both phenomenologically and with numerical simulations) is the appearance of ordered structures called *nuclear pasta phase* (see [1], [2], [3], [4], [5], [6], [7], [8], [9], [10], [11] and the nice up to date review [12]). Two of the most studied shapes are *nuclear spaghetti* (in which most of the Baryonic charge lies within tube-shaped region) and *nuclear lasagna* (in which most of the Baryonic charge lies within layers of finite width). In the present paper we will analyze in details these two types of nuclear pasta phase.

The properties of nuclear pasta attracted a lot of attention recently (see [6], [7], [8], [13], [14], [15] and references therein), but, due to both the very large Baryon number typical of this phase as well as to the strong interactions between them, only numerical results are available. Moreover, to obtain meaningful numerical results is extremely challenging in these complex systems and a very high computing power is required (as it can be deduced from the references mentioned above). Needless to say, it is usually assumed that any analytic approach is out of question. More in general, analytic tools (different from perturbation theory) to analyze the phase diagram of the low energy limit of Quantum Chromodynamics (QCD) at finite density and low temperatures are extremely rare (especially due to the non-perturbative nature of low energy QCD). This explains why the

interesting but complex phase diagram of QCD at finite density and low temperature is assumed to be out of reach of analytic techniques (see [16], [17], [18], [19] and references therein).

Nevertheless, the main aim of the present paper is *to present an analytic tool* suitable for the study of both, the nuclear spaghetti and nuclear lasagna phases, within the Skyrme model [20], which describes the low energy limit of QCD at the leading order in the 't Hooft expansion [21], [22], [23], [24], [25] (see also [26], [27] and references therein). The Skyrme model is a non-linear field theory for a scalar field U taking values in the $SU(N)$ Lie group, being N the flavor number. Despite the scalar nature of U , the solitons of the theory are interpreted as Baryons.

Of course, one may ask: *why should one insist so stubbornly in finding analytic solutions if these equations can be solved numerically?* In fact, the numerical tools in the references on nuclear pasta mentioned above are powerful enough to shed new light on this phase. However, there are indisputable reasons which compel us, whenever it is possible, to strive for analytic solutions nevertheless.

First of all, it could be enough to remind all the fundamental ideas that the Schwarzschild and Kerr solutions in General Relativity and the non-Abelian monopoles and instantons in Yang-Mills-Higgs theory disclosed. Consequently, an analytic tool to study the nuclear pasta phase can greatly enlarge our understanding of this complex phase. *Secondly and most importantly*, our analysis discloses relevant differences in the nuclear pasta phase arising from the competition between nuclear spaghetti and nuclear lasagna (which would have been hard to discover without the present analytic tools).

The methods introduced in [28], [29], [30], [31], [32], [33], [34], [35], [36], [37], [38] and [39] allowed the construction of several analytic and topologically non-trivial solutions of the Skyrme model at finite Baryon density. As far as the present paper is concerned, there are two relevant configurations analyzed in those references. *The first family* corresponds to ordered Baryonic arrays in which (most of) the topological charge and total energy are concentrated within tube-shaped regions¹. *The second family* corresponds to configurations in which (most of) the topological charge and total energy are concentrated within layers of finite width. Thus, the first family is suitable to describe nuclear spaghetti while the second family to describe nuclear lasagna. Indeed, on the nuclear spaghetti side, the similarity of the contour plots in [32] with the spaghetti-like configurations found (numerically) in the nuclear pasta phase (see the plots in [1], [2], [3], [4], [5] and [12]) is quite remarkable. On the nuclear lasagna side, the contour plots of the energy density and Baryon density, which can be found using the results in [31], are very close to the numerical plots in [1], [2], [3], [4], [5], for the lasagna case. Moreover, in [39] the shear modulus of lasagna configurations has been estimated analytically, the result being close to recent numerical studies in [7] and [11]. These results clearly show that the Skyrme model is suitable to describe the nuclear pasta phase both qualitatively and quantitatively. With only two exceptions in the

¹In [40] and [41], numerical string shaped solutions in the Skyrme model with mass term have been constructed. However, those configurations have a zero topological density (and they are expected to decay into Pions). The configurations analyzed in the present paper are topologically non-trivial and therefore can not decay into those of [40] and [41].

lasagna case (namely, [30] and [39]), all the analytic results useful for the nuclear pasta phase (namely [29], [31], [32], [33], [35], [36], [37], [38]) have been obtained in the case of the $SU(2)$ -Skyrme model.

In the present manuscript we will extend the results of all the above references to the case of the $SU(N)$ -Skyrme model for generic N . This is quite important from the viewpoint of the applications of the Skyrme model since in many concrete situations (such as the nuclear pasta phase) it could be relevant the inclusion of more flavors beyond Pions, Neutrons and Protons: in particular, the most relevant cases (beyond $N = 2$) are $N = 3$ and $N = 4$. Moreover, this generalization to generic N also allows to use the concept of non-embedded solutions (introduced in [23] and [24]) which are solutions of the $SU(N)$ -Skyrme model which cannot be written as trivial embeddings of $SU(2)$ in $SU(N)$. Thus, combining the strategy of [32], [33], [34], [36], [37], [39], with the generalization of the Euler angles to $SU(N)$ of [42], [43], [44], we will construct non-embedded multi-Baryonic solutions of nuclear spaghetti and nuclear lasagna.

The present analytic framework allows to write the explicit analytic formulas for the energy density and the total energy of these configurations for generic N , for large values of the Baryonic charge B and for each value of the size of the spatial volume within these configurations are living. One can compare the energy (seen as a function of the volume) of nuclear spaghetti with the energy of nuclear lasagna *for fixed values of the Baryonic charge and fixed N* : the result is that in the high density regime (but still well within the range of validity of the Skyrme model) the lasagna configurations are favored while at low density the spaghetti configurations are favored. In fact, the comparison between the magnetic field decay of neutron stars and their corresponding spin evolution obtained by numerical methods in references [45] and [46], suggests that such structures exist. In the light of the fact that lasagna and spaghetti phases are expected to have quite different physical properties (see [12] and references therein).

A possible criticism to the present analytic results is the following: all these configurations have been constructed with a careful choice of the ansatz for lasagna and spaghetti in the Skyrme case. In the 't Hooft expansion, one should expect subleading corrections to the Skyrme model (see, for instance, [47], [48], [49], [50] and [51]) which may spoil the present construction at subleading orders. However, the results in [34] strongly suggest that the same ansatz used in the present manuscript *allows to construct these configurations at any order in the 't Hooft expansion analytically, no matter how many subleading terms are included*.

The paper is organized as follows. In Section 2 we give a brief review of the $SU(N)$ -Skyrme model together with the general parameterization for the fundamental fields. In Section 3 we construct analytical solutions describing the nuclear spaghetti phase for generic values of N and we study its main features as the energy density distribution in terms of the Baryonic charge, the flavor number and density. In Section 4 we first review the nuclear lasagna phase and then we compare both configurations. Also we briefly discuss the large N limit of our configurations, the subleading corrections and the inclusion of a Isospin chemical potential. In the final Section some conclusions and perspectives will be presented.

2 The theory

In this section we briefly review the $SU(N)$ -Skyrme model that describes the low energy limit of QCD at the leading order in the 't Hooft expansion (see [20], [21], [22], [23], [24], [25], [26], [27] and references therein) and we present the general parameterization for the fields that will be used to construct topological soliton solutions.

2.1 The $SU(N)$ -Skyrme model

The action of the $SU(N)$ -Skyrme model in $(3+1)$ dimensions is

$$I = \int d^4x \sqrt{-g} \left[\frac{K}{4} \text{Tr} \left(R_\mu R^\mu + \frac{\lambda}{8} F_{\mu\nu} F^{\mu\nu} \right) \right] , \quad (2.1)$$

$$R_\mu = U^{-1} \nabla_\mu U , \quad F_{\mu\nu} = [R_\mu, R_\nu] , \quad U(x) \in SU(N) ,$$

where ∇_μ is the Levi-Civita covariant derivative, K and λ are positive coupling constants and g is the metric determinant. In our convention $c = \hbar = 1$ and Greek indices $\{\mu, \nu, \rho, \dots\}$ run over the four dimensional space-time with mostly plus signature. Latin indices $\{i, j, k, \dots\}$ are reserved for those of the internal space.

The Skyrme field U is a map over the space-time taking values in the $SU(N)$ Lie group (being N the flavor number), so that

$$R_\mu = R_\mu^i t_i ,$$

is in the $su(N)$ Lie algebra, where t_i are the infinitesimal generators of the $SU(N)$ group. We will see below that, for a given irreducible representation of the group, it is possible to construct analytic Baryonic configurations by deformations of embeddings of three dimensional Lie groups into $SU(N)$.

The field equations of the model are obtained varying the action in Eq. (2.1) w.r.t. the U field,

$$\nabla^\mu \left(R_\mu + \frac{\lambda}{4} [R^\nu, F_{\mu\nu}] \right) = 0 , \quad (2.2)$$

being these $(N^2 - 1)$ non-linear coupled second order differential equations.

The energy-momentum tensor, which is obtained using the standard formula

$$T_{\mu\nu} = -2 \frac{\partial \mathcal{L}}{\partial g^{\mu\nu}} + g_{\mu\nu} \mathcal{L} ,$$

turns out to be

$$T_{\mu\nu} = -\frac{K}{2} \text{Tr} \left(R_\mu R_\nu - \frac{1}{2} g_{\mu\nu} R_\alpha R^\alpha + \frac{\lambda}{4} (g^{\alpha\beta} F_{\mu\alpha} F_{\nu\beta} - \frac{1}{4} g_{\mu\nu} F_{\alpha\beta} F^{\alpha\beta}) \right) . \quad (2.3)$$

The topological charge is defined by

$$B = \frac{1}{24\pi^2} \int_\Sigma \rho_B , \quad \rho_B = \epsilon^{abc} \text{Tr} \left[(U^{-1} \partial_a U) (U^{-1} \partial_b U) (U^{-1} \partial_c U) \right] , \quad (2.4)$$

where $\{a, b, c\}$ are spatial indices. When the topological charge density ρ_B in Eq. (2.4) is integrated on a space-like surface, B turns out to be the Baryonic number². Since we are interested in describing states of Baryons, we need to impose that $\rho_B \neq 0$.

2.2 General parameterization

As one of our aims is the analysis of the finite density effects on the multi-solitons, we need to put the system within a box of finite volume. The simplest way to achieve this goal is to use the following flat metric

$$ds^2 = -dt^2 + L_r^2 dr^2 + L_\theta^2 d\theta^2 + L_\phi^2 d\phi^2 , \quad (2.5)$$

where the adimensional spatial coordinates have the ranges

$$0 \leq r \leq 2\pi , \quad 0 \leq \theta \leq 2\pi , \quad 0 \leq \phi \leq 2\pi , \quad (2.6)$$

so that the solitons are confined in a box of volume $V = (2\pi)^3 L_r L_\theta L_\phi$. It is worth to emphasize here a relevant point: The ranges in Eq. (2.6) are enforced by the theory of Euler angles for $SU(N)$ [42], [43], [44]. On the other hand, the constants L_r , L_θ and L_ϕ have dimensions of length. If one chooses physical unities such that $K = 1$ and $\lambda = 1$, then one would be measuring lengths in Fermi, fm . The natural units of density is $\rho \sim 1/(\text{volume})$.

A remark is in order. While more or less everybody agrees on the value of the coupling constant K , the value of λ is still under discussion. A typical way to fix λ is analyzing the properties of nucleons, as in [25]. However, the size of the Skyrme coupling can change depending on whether one focuses on the properties of a single nucleon or of nuclear matter; see the discussion in [27].

For the Skyrme field $U(x) \in SU(N)$ we use a parameterization in terms of the generalized Euler angles [42], [43], [44], that is

$$U = e^{\chi(x) (\vec{n} \cdot \vec{T})} , \quad (2.7)$$

$$\vec{n} = (\sin \Theta \sin \Phi, \sin \Theta \cos \Phi, \cos \Theta) , \quad (2.8)$$

where $\vec{T} = (T_1, T_2, T_3)$ are three matrices of a given representation of the Lie algebra $su(N)$, which will be chosen in order to satisfy (see Appendix A for more details) the following relations

$$[T_j, T_k] = \epsilon_{jkm} T_m , \quad \text{Tr}(T_j T_k) = -\frac{N(N^2 - 1)}{12} \delta_{jk} .$$

In principle the functions χ , Θ , Φ that appear in the ansatz in Eqs. (2.7) and (2.8) can depend on all the coordinates, but (in the next section) we will choose these functions in such a way to obtain analytical solutions with high topological charge. Then χ will be identified as the soliton profile.

²We will see below that the Baryonic number for both nuclear pasta phases depends explicitly on the flavor number N .

From Eqs. (2.4), (2.7) and (2.8) it follows that the topological charge density goes as

$$\rho_B \sim (\sin^2(\frac{\chi}{2}) \sin \Theta) d\chi \wedge d\Theta \wedge d\Phi , \quad (2.9)$$

and therefore, as we want to consider only topologically non-trivial configurations, we must demand that

$$d\chi \wedge d\Theta \wedge d\Phi \neq 0 . \quad (2.10)$$

It is important to note that Eq. (2.10) is a necessary but, in general, not sufficient condition. In the next section we will show the convenient form that the functions χ , Θ and Φ should take and the appropriate boundary conditions that lead to a non-vanishing topological charge identified as the Baryonic number.

3 Nuclear spaghetti phase

In this section we will show that the $SU(N)$ -Skyrme model admits analytical solutions describing crystals of Baryonic tubes (nuclear spaghetti phase) at finite volume.

3.1 The ansatz

We need a good ansatz that respect the condition in Eq. (2.10) to have a non-vanishing topological charge and also simplifies as much as possible the field equations in Eq. (2.2) in order to have analytic solutions describing Baryonic states. According to Eq. (2.2), a good set of conditions that allows to considerably simplify the field equations are

$$\nabla_\mu \Phi \nabla^\mu \chi = \nabla_\mu \chi \nabla^\mu \Theta = \nabla_\mu \Phi \nabla^\mu \Phi = \nabla_\mu \Theta \nabla^\mu \Phi = \square \Theta = \square \Phi = 0 . \quad (3.1)$$

Following the analysis in [32] and [33] one can see that a suitable choice that satisfies both of the above criteria (specified in Eqs. (2.10) and (3.1)) is the following:

$$\begin{aligned} \chi &= \chi(r) , \quad \Theta = q\theta , \quad \Phi = p \left(\frac{t}{L_\phi} - \phi \right) , \\ q &= \frac{1}{2}(2v+1) , \quad v \in \mathbb{N} , \quad p \neq 0 . \end{aligned} \quad (3.2)$$

It is worth to note here that p needs not to be an integer (as what is important is that both n and np should be integer where n is defined in Eq. (3.11) here below since n is related to the number of spaghetti in the box while np is related to the Baryon charge). As the analysis in the following sections will show, the energy-momentum tensor and the Baryon density do not depend on the coordinate ϕ while they do depend on r and θ (that's why these configurations describe nuclear spaghetti). Thus, p represents the Baryon number per unit of L_ϕ . Hence, intuitively, values of p less than 1 represents low Baryon density per unit of length while values greater than 1 represents high Baryon density per unit of length of spaghetti configurations.

The above ansatz has allowed the construction of crystals of Baryonic tubes as well as superconducting tubes in the $SU(2)$ -Skyrme model [32], [33], [34], [36]. Furthermore,

the ansatz in Eq. (3.2) has a sort of universal character since it allows to construct this kind of solutions also in the low energy limit of QCD [34], making it clear that no matter how many subleading terms in the 't Hooft expansion are additionally considered in the Skyrme action, the good properties of the above ansatz remain intact. That is the reason why we will use the ansatz in Eqs. (2.5), (2.7), (2.8) and (3.2) as a starting point for the construction of topological solitons in the $SU(N)$ case.

On the other hand, the matrices T_i define a three dimensional subalgebra of $su(N)$ (see for example Appendix D of [39]) and are given explicitly as

$$T_1 = -\frac{i}{2} \sum_2^N \sqrt{(j-1)(N-j+1)} (E_{j-1,j} + E_{j,j-1}) , \quad (3.3)$$

$$T_2 = \frac{1}{2} \sum_2^N \sqrt{(j-1)(N-j+1)} (E_{j-1,j} - E_{j,j-1}) , \quad (3.4)$$

$$T_3 = i \sum_1^N \left(\frac{N+1}{2} - j \right) E_{j,j} , \quad (3.5)$$

with

$$(E_{i,j})_{mn} = \delta_{im} \delta_{jn} ,$$

being δ_{ij} the Kronecker delta (see Appendix A for more mathematical details).

3.2 Solving the system analytically

It is a direct computation to verify that, according to the ansatz defined in Eqs. (2.5), (2.7), (2.8) and (3.2), the components of the tensor R_μ are

$$\begin{aligned} R_t &= \frac{p}{L_\phi} (\sin \chi \tau_3 + (1 - \cos \chi) \tau_2) \sin(q\theta) , \\ R_r &= \chi' \tau_1 , \\ R_\theta &= q (\sin \chi \tau_2 - (1 - \cos \chi) \tau_3) , \\ R_\phi &= -L_\phi R_t , \end{aligned}$$

while the non-vanishing components of $F_{\mu\nu}$ turns out to be

$$\begin{aligned} F_{tr} &= \frac{p}{L_\phi} (\sin \chi \tau_2 - (1 - \cos \chi) \tau_3) \chi' \sin(q\theta) , \\ F_{t\theta} &= -\frac{2pq}{L_\phi} (1 - \cos \chi) \sin(q\theta) \tau_1 , \\ F_{r\theta} &= q (\sin \chi \tau_3 + (1 - \cos \chi) \tau_2) \chi' , \\ F_{r\phi} &= L_\phi F_{tr} , \\ F_{\theta\phi} &= L_\phi F_{t\phi} , \end{aligned}$$

where

$$\tau_1 = \vec{n} \cdot \vec{T} , \quad \tau_2 = \partial_\Theta \tau_1 , \quad \tau_3 = \frac{1}{\sin \Theta} \partial_\Phi \tau_1 , \quad [\tau_i, \tau_j] = \varepsilon_{ij}^k \tau_k .$$

From the above, the $(N^2 - 1)$ coupled field equations of the Skyrme model in Eq. (2.2) with the ansatz defined in Eqs. (2.5), (2.7) and (3.2) are reduced to just one single ODE for the profile χ , namely

$$\left(1 + \frac{\lambda q^2}{L_\theta^2} \sin^2\left(\frac{\chi}{2}\right)\right) \chi'' - \frac{q^2 L_r^2}{L_\theta^2} \left(1 - \frac{\lambda}{4 L_r^2} \chi'^2\right) \sin(\chi) = 0 . \quad (3.6)$$

Note that Eq. (3.6) does not depend on N , so that the Skyrme equation is independent of the Lie group under consideration³. Furthermore, the above equation can be reduced to the following first order ODE

$$\left(1 + \frac{q^2 \lambda}{L_\theta^2} \sin^2\left(\frac{\chi}{2}\right)\right) \chi'^2 + \frac{2 L_r^2 q^2}{L_\theta^2} \cos(\chi) = E_0 , \quad (3.7)$$

where E_0 is an integration constant. Eq. (3.7) is explicitly solvable in terms of generalized Elliptic Integrals [52] and it is reducible to the following quadrature

$$\frac{d\chi}{\eta(\chi, E_0)} = \pm dr , \quad \eta(\chi, E_0) = \pm \left[\frac{E_0 L_\theta^2 - 2 L_r^2 q^2 \cos(\chi)}{L_\theta^2 + q^2 \lambda \sin^2(\frac{\chi}{2})} \right]^{\frac{1}{2}} . \quad (3.8)$$

The integration constant E_0 plays a fundamental role in determining the Baryonic charge, as we will see here below.

3.3 A constraint from stability

When the field equations reduce to a single equation for the profile in a topologically non-trivial sector (as in the present case) one says that “*the hedgehog property holds*”. Often (although not always, see [53], [54] and references therein) the most dangerous perturbations⁴ are those perturbations of the profile which keep the hedgehog property.

In the present case, these dangerous perturbations are of the following form:

$$\chi \rightarrow \chi + \varepsilon \xi(r) , \quad |\varepsilon| \ll 1 , \quad (3.9)$$

which do not change the $SU(N)$ Isospin degrees of freedom but only the profile. It is a direct computation to show that the linearized field equations under the perturbation in Eq. (3.9) always has the following zero-mode: $\xi(r) = \partial_r \chi(r)$, where χ is the solution of the field equations (satisfying the boundary conditions defined here below). From this we can deduce a constraint (which is a necessary condition for stability) on the integration

³We will see below that, although the profile does not depend on N , both the energy and the Baryonic charge are functions of N , as expected.

⁴Namely, a perturbation which could lead to a decrease in the energy of the system.

constant E_0 in Eqs. (3.7) and (3.8), namely

$$E_0 > \frac{2L_r^2 q^2}{L_\theta^2}.$$

If the above condition is satisfied the zero mode $\xi(r) = \partial_r \chi(r)$ has no node (since $\partial_r \chi(r)$ does not vanish in this case) and so the system is stable under these perturbations.

3.4 Boundary conditions and Baryonic charge

From Eq. (2.4) and using Eqs. (2.7), (2.8) and (3.2) we can compute the topological charge density of the configurations presented above, which turns out to be

$$\rho_B = N(N^2 - 1) pq \sin(q\theta) \sin^2\left(\frac{\chi}{2}\right) \chi'. \quad (3.10)$$

We see that, in fact, the topological charge density depends on the Lie group through the factor $N(N^2 - 1)$. Integrating the above over a space-like hypersurface in the ranges defined in Eq. (2.6), we arrive to the following expression for the topological charge

$$B = 2np \frac{N(N^2 - 1)}{12}, \quad (3.11)$$

where we have used the following boundary conditions

$$\chi(0) = 0, \quad \chi(2\pi) = 2n\pi, \quad (3.12)$$

with n an integer and q specified in Eq. (3.2). These conditions arise if we require the U field to cover an entire cycle in the range of the coordinates in Eq. (2.6). As shown in [43], this is accomplished imposing that the variables explicitly appearing in the “measure” in Eq. (3.10) must run in a range where the measure is non-vanishing. This fact immediately implies that $\theta \in [0, \pi/q]$ (for a fundamental solution) and $\chi \in [0, 2\pi]$. Therefore the topological charge for the spaghetti phase depends on N and it is labeled by the integer n that appears in the boundary conditions in Eq. (3.12) and the value of p in the ansatz in Eq. (3.2). Note that the integration constant E_0 in Eq. (3.8) is fixed in terms of n through the equation

$$n \int_0^{2\pi} \frac{1}{\eta(\chi, E_0)} d\chi = 2\pi, \quad (3.13)$$

that will always have a real solution.

We want to remark here that, despite our choice of the ranges may look to define periodic boundary conditions, it is not the case. The boundary conditions are chosen so that the map embedding the spatial rectangle into the $SU(N)$ exactly wraps a cycle in $H_3(SU(N), \mathbb{Z})$. This is a topological condition necessary to have a non vanishing Baryon number, while it is easy to see that periodic boundary conditions in all variables would lead to a vanishing Baryon number (see [42, 43]).

3.5 Characterizing the $SU(N)$ nuclear spaghetti phase

At this point it is important to emphasize that using the ansatz introduced in Section 3.1 we have reduced the complete set of Skyrme equations to just one equation in Eq. (3.6) for the profile χ . Even more, this equation can be solved analytically and does not depend on N .

In what follows we will set the values of the coupling constants as $K = 2$ and $\lambda = 1$ for the numerical computations. We will also define the density in the case $L_r = L_\theta = L_\phi \equiv L$, as $\rho = 1/(2\pi L)^3$.

Fig. 1 shows the behavior of the profile of the soliton configurations as a function of the parameter n , which determines different values of the Baryonic charge according to Eq. (3.11). Now, even though the Skyrme equation does not depend on N explicitly (see Eq.

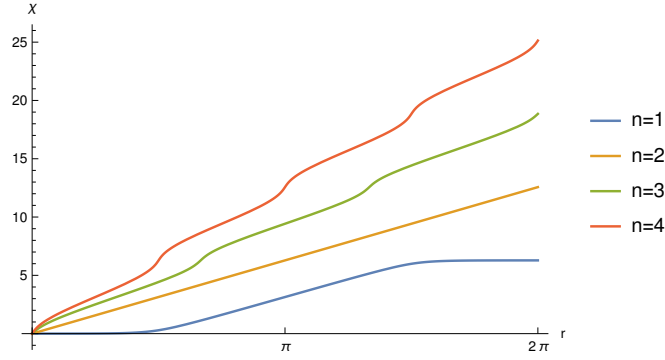


Figure 1: Soliton profile $\chi = \chi(r)$ for different values of n , with $q = \frac{9}{2}$ and $L = 1$.

(3.6)), the energy density does. In fact, according to Eq. (4.16) and using Eqs. (2.5), (2.7) and (3.2), the energy density of these configurations is

$$\mathcal{E} = \frac{K}{4} \frac{N(N^2 - 1)p}{12L_r L_\theta L_\phi^2} (\rho_0 + 2 \sin^2(q\theta)\rho_1) , \quad (3.14)$$

where the functions ρ_0 and ρ_1 are given respectively by

$$\begin{aligned} \rho_0 &= \frac{L_\phi^2}{p} \left[4L_r^2 q^2 \sin^2\left(\frac{\chi}{2}\right) + \left(L_\theta^2 + q^2 \lambda \sin^2\left(\frac{\chi}{2}\right) \right) \chi'^2 \right] , \\ \rho_1 &= p \sin^2\left(\frac{\chi}{2}\right) \left[4L_r^2 \left(L_\theta^2 + q^2 \lambda \sin^2\left(\frac{\chi}{2}\right) \right) + L_\theta^2 \lambda \chi'^2 \right] . \end{aligned}$$

In Fig. 2 we show plots of the energy density for some of the allowed spaghetti configurations with $B = 4$, which is the lowest value of the topological charge in both $N = 2$ and $N = 3$ cases according to Eq. (3.11) (see Table 1 in Appendix B for the explicit values of $B = B(N)$) when both, the value of the parameters q and n increase. We see that the number of peaks in the r direction increases as n increases, while the value of the parameter q repeats the pattern in the θ direction of the lattice in which the solitons are confined.

In Fig. 3, in the left side, we have plotted the total energy as a function of the

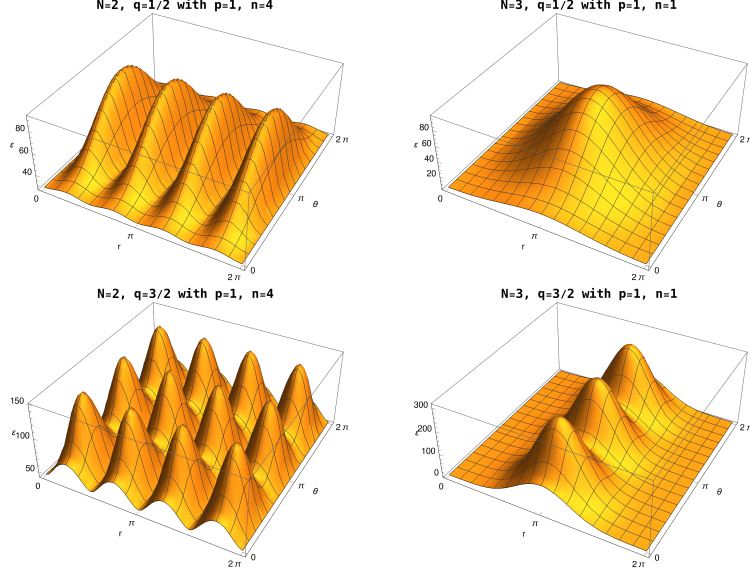


Figure 2: Energy density for some of the allowed configurations with $B = 4$ for different values of q and with $p = 1$ and $L = 1$.

Baryonic charge for different fixed values of the flavor number. In the right side we show the behavior of the total energy in terms of the flavor number once fixed the topological charge. From here we can see two interesting facts: when the value of N is fixed the energy is an increasing function of B . In the opposite way, when a particular value of B is chosen, the energy decreases with N . This means that if we consider a fixed volume box, as we add more Baryons to the box the energy of the system increases, which is the expected result due to the repulsion energy between Baryons. Now, if we compare the same fixed volume box containing the same Baryonic number but for different values of the group dimension, as we increase N the energy of the configuration will be lower. According to the above, for example, the 4-Baryon state for the $SU(3)$ group in Fig. 2 (up-right) is less energetic than the four independent Baryons state for the $SU(2)$ group in Fig. 2 (up-left). The amount of energy per Baryon has the same behavior.

In Fig. 4 we show the behavior of the energy as the density changes; this for fixed values of B and N and considering a cubic box in which the solutions are confined. We can see that in the high density sector the energy of the system increases, being the divergence at the end expected since at low scales the Skyrme model (which is an effective model of Baryons and Pions) should be replaced by QCD. However, there is a critical point from which the behavior reverses in such a way that at low density the energy of the system becomes a decreasing function of the density. This “u-shaped” behavior of the energy versus density that we can see from Fig. 4 is in accordance with what has been obtained in numerical simulations of nuclear pasta (see [12]). In fact, the above is one of the main goals of the present work: relevant features of the nuclear pasta state, that until now has only been possible to study numerically, can be characterized from analytical solutions of the $SU(N)$ -Skyrme model.

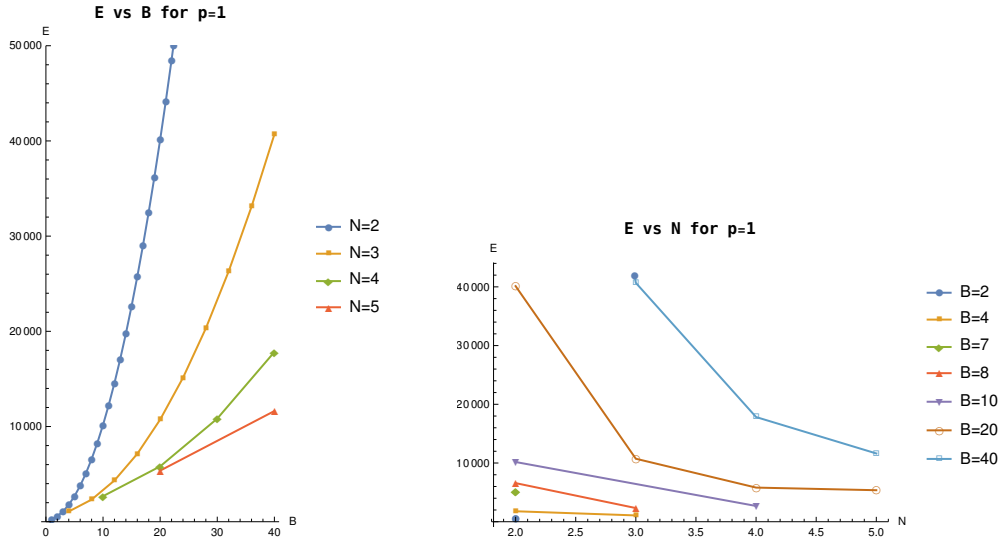


Figure 3: Left: Energy versus Baryonic charge for different values of N . Right: Energy versus N for different values of B . Here $p = 1$, $q = \frac{1}{2}$ and $L = 1$.

Fig. 5 shows that, for different configurations of nuclear spaghetti with the same Baryonic charge, there are transitions that depend on the values of the constants p and n that define the topological charge according to Eq. (3.11). In particular, from the left plot we see that at low densities the energetically preferable spaghetti configuration is the one with two flavors, whereas at larger densities the configuration with three flavors has the lowest energy. Also, from the right plot and for larger densities we can see a transition between spaghetti configurations within the same internal group ($N = 2$), for different values of p and n .

The following comment is in order. Traditionally (see, for instance, [25]) the Skyrme coupling constant is fixed by requiring the best possible agreement with the static properties of the Neutron and Δ_{++} . However (while everybody agrees on the Pions coupling constant K) there is no common agreement yet on the value of the Skyrme coupling constant λ . In the plot in Fig. 5 we have used the “traditional value” for the Skyrme coupling constant λ . On the other hand, it could be convenient to fix λ in order to get an excellent description of nuclear pasta. We think that the present results strongly support this point of view.

Finally, there is also a transition that appears when the value of the q parameter varies. In fact, from Fig. 6 we can see that as the density decreases the configurations with higher values of q becomes the energetically favored ones.

4 Nuclear spaghetti versus nuclear lasagna

In this section we will compare the nuclear spaghetti and nuclear lasagna phases.

4.1 Review of the $SU(N)$ nuclear lasagna phase

Here we will summarize the most important features of the nuclear lasagna solutions that were previously constructed in [39], in order to compare these solutions with the new

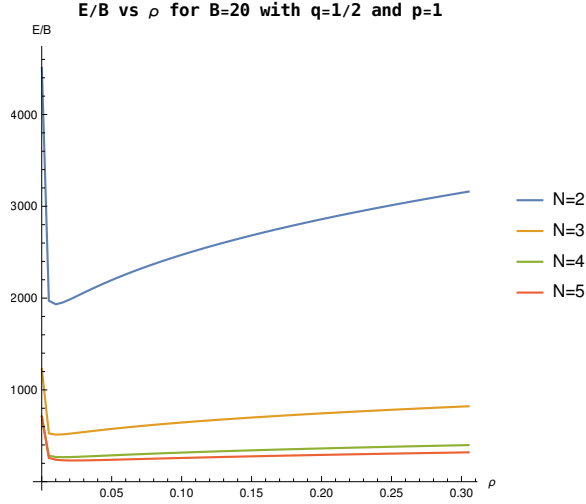


Figure 4: Energy per Baryonic charge as a function of the density with $q = \frac{1}{2}$. We show all the allowed configurations with $B = 20$ and $p = 1$. One can see that the behavior of the curves has the characteristic “u-shape” of nuclear pasta shown in [12].

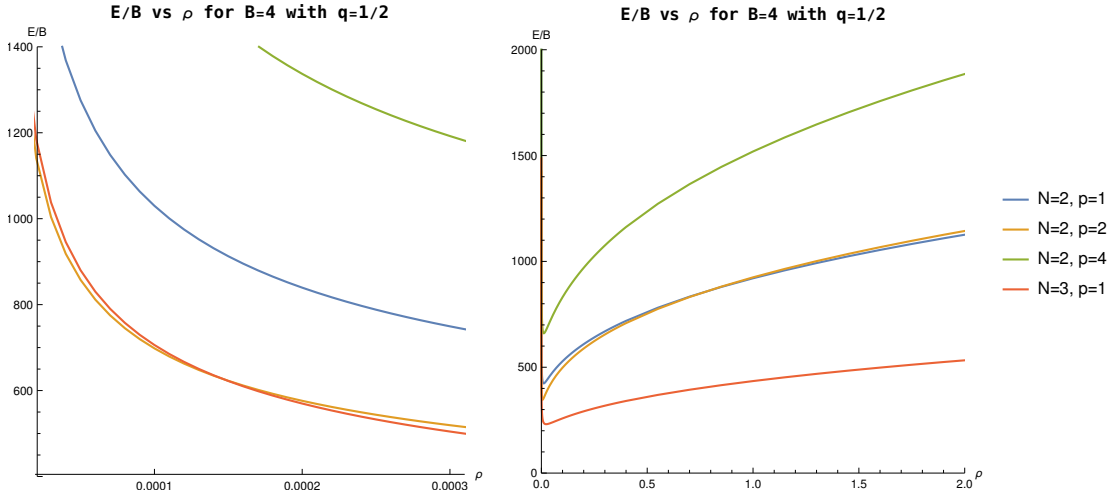


Figure 5: Energy per Baryonic charge as a function of the density with $q = \frac{1}{2}$. For $B = 4$ we see (when N , p and n varies) left: At low densities the energetically preferable spaghetti configuration in $N = 2$, whereas at larger densities the configuration with $N = 3$ has the lowest energy. Right: We see a transition that occurs between configurations with $N = 2$, for different values of n and p .

nuclear spaghetti phase presented in the previous section of this manuscript.

The ansatz for the Skyrme field that allows to construct the analytic nuclear lasagna phase, as a solution of the $SU(N)$ -Skyrme model in Eqs. (2.1) and (2.2), is given by

$$U_L = e^{\sigma \Phi k} e^{h(r)} e^{m \theta k} , \quad (4.1)$$

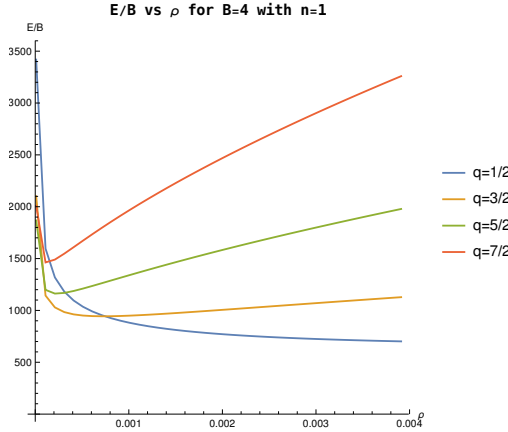


Figure 6: Energy per Baryonic charge as function of the density with $B = 4$ in $SU(2)$ and for different values of q . We see that, at high density, configurations with lower values of q are energetically favoured while, in the low density sector, the configurations with higher values of q are the favoured ones.

where

$$\sigma = 2^{-\frac{(-1)^N + 1}{2}}, \quad \Phi = \frac{t}{L_\phi} - \phi, \quad k = \sum_{j=1}^{N-1} \left(c_j E_{j,j+1} - c_j^* E_{j+1,j} \right). \quad (4.2)$$

Here m is a non-vanishing integer number and c_j are arbitrary complex numbers with the constraint that $e^{\theta k}$ must be periodic with period 2π . The last is indeed a highly nontrivial constraint, which has been solved in [39]. We will consider again the metric of a box in Eq. (2.5) with the same ranges in the coordinates.

It is worth to remark that in [39] it has been shown that the solutions of such constraints define a moduli space (the set of allowed c_j) which becomes larger and larger with N . For a generic choice of c_j , and thus of k , in such moduli space, the linear space generated by the matrices $h(r), k$ and $[h(r), k]$ is not a tridimensional subalgebra of $su(N)$. This happens only by choosing the parameters c_j in a subset of vanishing measure of the moduli space. This means that for a generic choice of the parameters, despite expression (4.1) has the form of an Euler parametrization of $SU(2)$, it does not define a subgroup of $SU(N)$, but just a submanifold. In this sense the Euler construction is not an embedding of $SU(2)$ into $SU(N)$ as Lie groups, but only as manifolds. Remarkably, the very specific choices that give rise to embeddings of $SU(2)$ in $SU(N)$ (and other simple Lie groups) have been determined by E. Dynkin in [59]. In the very particular cases (which are instead the general case for the spagetti construction) when the choice of the parameters defines a subgroup, then we have an embedding which is called non-trivial if the image contains sub representations of spin different from 0 and $1/2$, and trivial otherwise. In the non trivial case, one usually says that the corresponding solutions of the Skyrme equations are of true $SU(N)$ type (see [39] and references therein).

It can be directly checked that the configurations described by the ansatz in Eqs. (2.5) and

(4.1) reduce the complete set of Skyrme field equation (see [39] for details) to the following ODE:

$$h'' = \frac{\lambda q^2}{4L_\gamma^2} ([k, [k, h'']] - [k, [h', [h', k]]]) . \quad (4.3)$$

Eq. (4.3) can be directly solved, and its solution is given by

$$h(r) = \frac{1}{2} r v_\varepsilon , \quad v_\varepsilon = \sum_{j,k} C_{A_{N-1} j, k}^{-1} \varepsilon_k J_j , \quad (4.4)$$

where ε_j are signs, with $\varepsilon_1 = 1$ and $C_{A_{N-1}}$ is the Cartan matrix for $SU(N)$ (see [39], Proposition 2). Here, J_j form a basis of the Cartan subalgebra of $SU(N)$ defined as

$$J_j = i(E_{j,j} - E_{j+1,j+1}) .$$

It follows that the energy density for the nuclear lasagna phase is given by

$$\begin{aligned} T_{00} = & -\frac{K}{2} L_\phi^2 \text{Tr} \left[R_t^2 + \frac{1}{2} \left(\frac{R_r^2}{L_r^2} + \frac{R_\theta^2}{L_\theta^2} \right) + \frac{\lambda}{4} \left(\frac{F_{tr}^2}{L_r^2} + \frac{F_{t\theta}^2}{L_\theta^2} + \frac{1}{2} \frac{F_{r\theta}^2}{L_r^2 L_\theta^2} \right) \right] \\ = & \frac{K}{2} \|c\|^2 L_\phi^2 \left(\frac{m^2}{L_\theta^2} + \frac{1}{8L_r^2} \frac{\|v_\varepsilon\|^2}{\|c\|^2} + 2 \frac{\sigma^2}{L_\phi^2} + \frac{\lambda m^2}{16L_r^2 L_\theta^2} + \frac{\lambda \sigma^2}{8L_\phi^2 L_r^2} \right) \\ & + \frac{K \lambda m^2 \sigma^2}{L_\theta^2} \sin^2 \left(\frac{r}{2} \right) \left(\sum_{j=1}^{N-1} |c_j|^4 + \sum_{j=1}^{N-2} |c_j|^2 |c_{j+1}|^2 \left(\frac{1}{2} - \frac{3}{2} \varepsilon_j \varepsilon_{j+1} \right) \right) , \quad (4.5) \end{aligned}$$

where we have denoted

$$\|c\|^2 = \sum_{j=1}^{N-1} |c_j|^2 , \quad \|v_\varepsilon\|^2 = -\text{Tr } v_\varepsilon^2 .$$

On the other hand the topological charge is

$$B_L = 2m\sigma \|c\|^2 . \quad (4.6)$$

In particular, we are interested in the case when $\varepsilon_j = 1$ for all j , so that

$$\begin{aligned} \|c\|^2 = \Lambda \|v_\varepsilon\|^2 &= \frac{\Lambda}{12} N(N^2 - 1) , \\ \sum_{j=1}^{N-1} |c_j|^4 - \sum_{j=1}^{N-2} |c_j|^2 |c_{j+1}|^2 &= \frac{\Lambda}{2} \|c\|^2 , \end{aligned}$$

where $\Lambda = \frac{1}{2}$ for odd N and $\Lambda = 2$ for even N (see Appendix B for the allowed values of the Baryonic charge as function of N).

Fig. 7 shows how the energy density changes for different values of the topological charge and for fixed values of N . Although the behavior of the energy density per Baryon is similar, the quotient E/B does not depend on N .

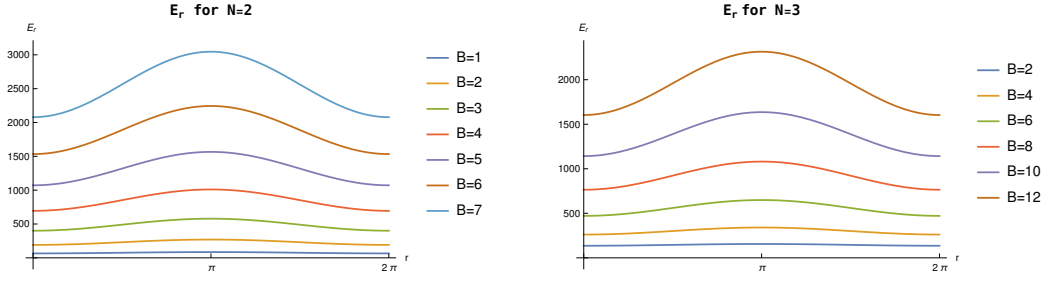


Figure 7: Energy density in r for the lasagna phase for $N = 2, 3$ and different values of B . Here $L = 1$ and $q = \frac{1}{2}$.

In Fig. 8 one can see that the lasagna phase has the same behavior as the spaghetti phase; its energy is an increasing quantity in B , and that lasagna configurations belonging to theories with lower N are more energetic than those with larger N values.

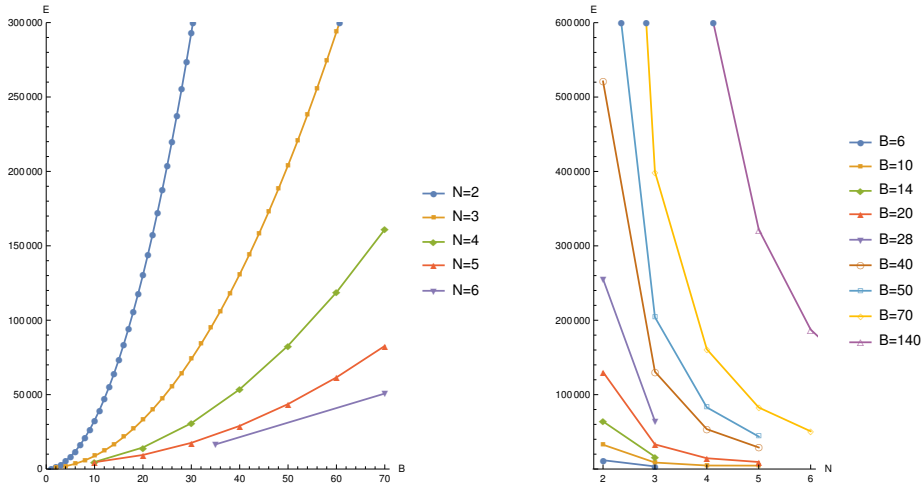


Figure 8: Energy per Baryonic charge versus B and energy versus N for the lasagna phase and for different values of N and B , respectively. Here $L = 1$ and $q = \frac{1}{2}$.

4.2 Comparing nuclear spaghetti and lasagna at finite Baryon density

In this subsection, we will compare the energy densities of the lasagna and spaghetti configurations.

First of all, it is important to note a key difference between the expressions for the topological charge of the lasagna and the spaghetti phases. Even though both configurations depends on the group dimension N (see Appendix B), the spaghetti phase also depends on two more integers, namely n and p (see Eq. (3.11)), while the lasagna depends only on the integer m (see Eq. (4.6)). Since we must compare configurations with the same Baryonic charge, for a given value of N , in the case of the spaghetti there will be many configurations that satisfy this requirement, while for the lasagna phase there will be only one.

According to the expressions for the energy of the spaghetti and lasagna phases in Eqs. (3.14) and (4.5), respectively, one can see that when the total energy (for fixed values of the Baryonic charge and fixed flavor number) is computed as a function of the density, at high density (but still well within the range of validity of the Skyrme model) the lasagna configurations are energetically favored while at low density the spaghetti configurations are favored (see Fig. 9).

It is also important to note that the q parameter present in the spaghetti-like configurations plays a very important role as $2qn$ represents the number of spaghetti in the box.

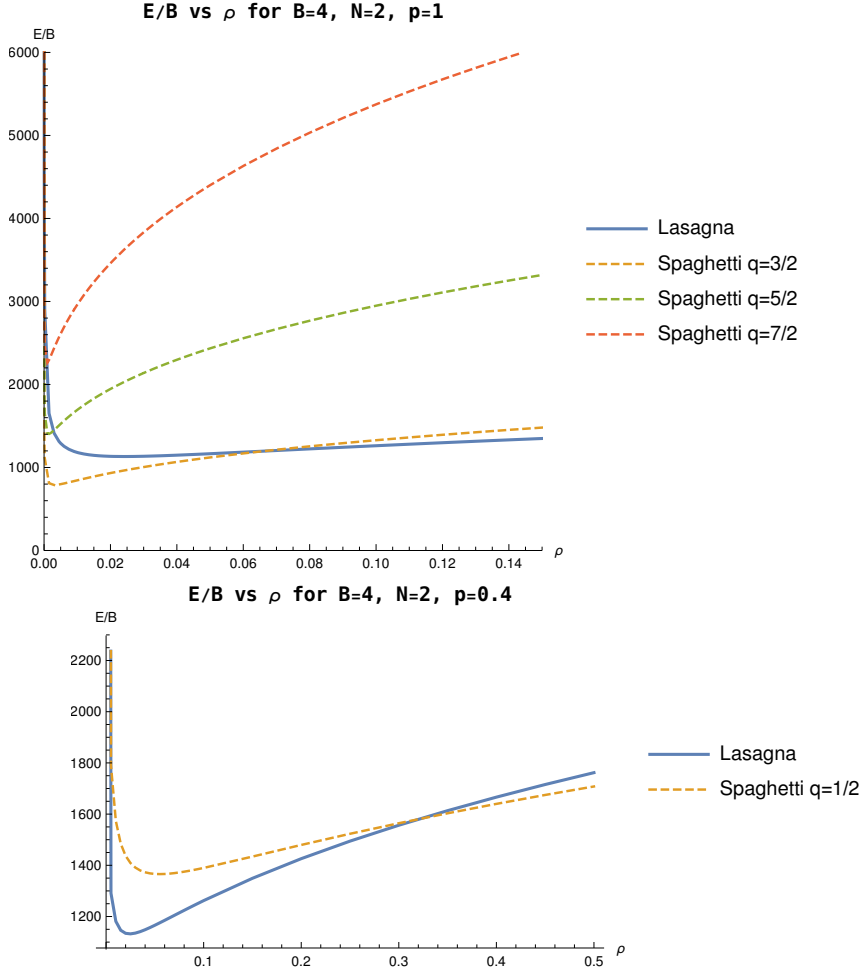


Figure 9: Energy per Baryonic charge of the nuclear pasta phases as a function of the density for different values of q . Above: For $p = 1$, we can see that below a certain value of ρ the spaghetti phase has a lower energy cost, while above this value the lasagna phase is the energetically desirable. Note that the lasagna phase also exhibits the characteristic “u-shape” behavior shown in [12]. Below: For $p = 0.4$ and $q = \frac{1}{2}$, we see that for low densities the lasagna phase has a lower energy cost, while for high density the spaghetti phase is the energetically favored.

From Fig. 9 it can be seen that the q parameter plays a very important role, as can also be seen from the plots. Indeed, the plot in Fig. 9 confirms that at high density lasagna configurations are energetically favoured while at low density spaghetti configurations are energetically favoured (the density at which one type of configuration overcomes the other depends on the parameter q).

4.3 A comment on the large N limit

Although the large N limit of the $SU(N)$ -Skyrme model is not directly relevant in the phenomenology of nuclear pasta, it has a great theoretical interest since it is connected with the Veneziano limit of the large N_c expansion of QCD, N_c being the number of colors, in which also the flavor number N goes to infinity keeping constant N/N_c (see [55], [56] and [57]). Here below we present a result that is of interest in this context (in which it is always an important achievement to show that physically meaningful quantities do possess a smooth large N limit). The energy per Baryon, $g(B, N, L) = E/B$, for the spaghetti and lasagna phases are given respectively by

$$g_S(B, N, L) = \frac{L^3 K (2\pi)^2}{8np} \left[4\xi_1(q^2 + p^2) + n^2\xi_4 + \frac{\lambda}{L^2} (n^2\xi_3(q^2 + p^2) + 4\xi_2 q^2 p^2) \right] , \quad (4.7)$$

$$g_L(B, N, L) = \frac{L^3 K (2\pi)^3}{2\sigma m} \left[m^2 + \frac{1}{8\Lambda} + 2\sigma^2 + \frac{\lambda}{L^2} \left(\frac{m^2}{16} + \frac{\sigma^2}{8} + \frac{\Lambda m^2 \sigma^2}{2} \right) \right] , \quad (4.8)$$

where we have defined the integrals

$$\xi_1 = \int_0^{2\pi} \sin^2 \left(\frac{\chi(r)}{2} \right) dr , \quad (4.9)$$

$$\xi_2 = \int_0^{2\pi} \sin^4 \left(\frac{\chi(r)}{2} \right) dr , \quad (4.10)$$

$$\xi_3 = \frac{1}{n^2} \int_0^{2\pi} \sin^2 \left(\frac{\chi(r)}{2} \right) \eta(r)^2 dr , \quad (4.11)$$

$$\xi_4 = \frac{1}{n^2} \int_0^{2\pi} \eta(r)^2 dr , \quad (4.12)$$

and $\eta(r)$ is defined in Eq. (3.8) (here, ξ_j do not scale with N). A fact that can be seen explicitly from our analytical construction is that the above quantities do not depend on N in a “significant way”. In particular, the energy per Baryon for the spaghetti case in Eq. (4.7) does not depend on N at all, while for the lasagna case in Eq. (4.8) the dependence is stored in the definition of Λ and σ and it takes different finite values depending on whether N is even or odd. Consequently, we have shown that the energy per Baryon $g_S(B, N, L)$ in the spaghetti case has a smooth well defined large N limit. In the lasagna case, $g_L(B, N, L)$ also possesses a well defined large N limit provided we treat separately the case in which N is large and even and the case in which N is large and odd.

4.4 Subleading corrections

In previous sections we mentioned that the configurations shown in this work are also solutions of the generalized Skyrme model including higher order corrections in the 't Hooft limit. It is worth to emphasize that this claim could appear to be quite unrealistic due to the extremely complex nature of the subleading corrections to the Skyrme model arising in the 't Hooft expansion [48]. Indeed, until very recently not only there was no analytic and topologically non-trivial solution of the Skyrme field equations modified by the corrections presented in [48], but such corrections were neglected also in the numerical analysis due to their highly non-linear character.

In fact, in [34] it was shown explicitly how such corrections modify the analytic spaghetti configurations for the $SU(2)$ group. In order to expand these results, in this subsection we will explicitly show a similar result for the lasagna phase in the cases of most physical interest: namely, for the internal groups with $N = 2$ and $N = 3$.

In four dimensions, we have that the low energy limit of QCD at leading order in the 't Hooft expansion can be described by the following action:

$$\hat{I} = I + \int d^4x \sqrt{-g} \mathcal{L}_{\text{corr}} , \quad (4.13)$$

where I corresponds to the Skyrme action defined above in Eq. (2.1) and the terms $\mathcal{L}_{\text{corr}}$ represents the possible subleading corrections to the Skyrme model which can be computed, in principle, using either Chiral Perturbation Theory (see [58] and references therein) or the large N expansion [55], [57]. The expected corrections have the following generic form

$$\begin{aligned} \mathcal{L}_6 &= \frac{c_6}{96} \text{Tr} [F_\mu^\nu F_\nu^\rho F_\rho^\mu] , \\ \mathcal{L}_8 &= -\frac{c_8}{256} \left(\text{Tr} [F_\mu^\nu F_\nu^\rho F_\rho^\sigma F_\sigma^\mu] - \text{Tr} [\{F_\mu^\nu, F_\rho^\sigma\} F_\nu^\rho F_\sigma^\mu] \right) , \end{aligned} \quad (4.14)$$

and so on [48], where the c_p ($p \geq 6$) are subleading with respect to K and λ .

The field equations of the model are obtained varying the action in Eq. (4.13) w.r.t. the U field. To perform this derivation it is useful to keep in mind the following relation

$$\delta_U R_\mu = [R_\mu, U^{-1} \delta U] + \partial_\mu (U^{-1} \delta U) ,$$

where δ_U denotes variation w.r.t the U field. From the above, the field equations of the generalized Skyrme model turns out to be

$$\begin{aligned} & \frac{K}{2} \left(\partial^\mu R_\mu + \frac{\lambda}{4} \partial^\mu [R^\nu, F_{\mu\nu}] \right) + 3c_6 [R_\mu, \partial_\nu [F^{\rho\nu}, F_\rho^\mu]] \\ & + 4c_8 \left[R_\mu, \partial_\nu \left(F^{\nu\rho} F_{\rho\sigma} F^{\sigma\mu} + F^{\mu\rho} F_{\rho\sigma} F^{\nu\sigma} + \{F_{\rho\sigma}, \{F^{\mu\rho}, F^{\nu\sigma}\}\} \right) \right] = 0 . \end{aligned} \quad (4.15)$$

On the other hand the energy-momentum tensor of the theory including the subleading corrections is

$$T_{\mu\nu} = T_{\mu\nu}^{\text{Sk}} + T_{\mu\nu}^{(6)} + T_{\mu\nu}^{(8)} , \quad (4.16)$$

where a direct computation reveals that

$$T_{\mu\nu}^{(6)} = -\frac{c_6}{16} \text{Tr} \left(g^{\alpha\gamma} g^{\beta\rho} F_{\mu\alpha} F_{\nu\beta} F_{\gamma\rho} - \frac{1}{6} g_{\mu\nu} F_{\alpha}^{\beta} F_{\beta}^{\rho} F_{\rho}^{\alpha} \right) ,$$

$$T_{\mu\nu}^{(8)} = \frac{c_8}{32} \text{Tr} \left(g^{\alpha\rho} g^{\beta\gamma} g^{\delta\lambda} F_{\alpha\mu} F_{\nu\beta} F_{\gamma\delta} F_{\lambda\rho} + \frac{1}{2} \{F_{\mu\alpha}, F_{\lambda\rho}\} \{F_{\beta\nu}, F_{\gamma\delta}\} g^{\alpha\gamma} g^{\beta\rho} g^{\delta\lambda} \right. \\ \left. - \frac{1}{8} g_{\mu\nu} (F_{\alpha}^{\beta} F_{\beta}^{\rho} F_{\rho}^{\sigma} F_{\sigma}^{\alpha} - \{F_{\alpha}^{\beta}, F_{\rho}^{\sigma}\} F_{\beta}^{\rho} F_{\sigma}^{\alpha}) \right) .$$

Now, considering the very same ansatz for the lasagna phase given in Eqs. (4.1) and (4.2) we obtain that the complete set of coupled Skyrme field equations reduce the single integrable ODE for the $SU(2)$ and $SU(3)$ cases, respectively

$$\left(16K L_r^2 L_{\theta}^2 (4L_{\theta}^2 + m^2 \lambda) - 3c_8 m^4 h'^2 \right) h'' = 0 , \quad (4.17)$$

$$\left(4K L_r^2 L_{\theta}^2 (4L_{\theta}^2 + m^2 \lambda) - 3c_8 m^4 h'^2 \right) h'' = 0 . \quad (4.18)$$

We write the field equations in this way in order to make clear that the inclusion of these corrections keep intact the nice structure of the field equations. It is also quite manifest that the lasagna solutions presented in this work, when the profile $h(r)$ is a linear function as in Eq. (4.4), also satisfy the field equations of this generalized model. This is a quite remarkable result in itself since, until very recently, such corrections were not even included in numerical analysis while with the present approach can be studied analytically.

Now, despite the fact that the high order corrections do not affect the structure of the field equations, these terms do play a role in the physical properties of these configurations. In particular, the energy density of this phase will be modified according to

$$T_{00}^{(6)} = \frac{1}{128} \frac{c_6 m^2}{L_r^2 L_{\theta}^2 L_{\phi}^2} \sin^2\left(\frac{r}{2}\right) , \quad T_{00}^{(8)} = \frac{1}{2^{14}} \frac{c_8 m^2}{L_r^4 L_{\theta}^4 L_{\phi}^2} \left(8L_{\theta}^2 + (8L_r^2 - L_{\phi}^2) m^2 + 4(L_{\theta}^2 - 2L_r^2 m^2) \cos(r) \right) ,$$

for $SU(2)$ and

$$T_{00}^{(6)} = \frac{1}{32} \frac{c_6 m^2}{L_r^2 L_{\theta}^2 L_{\phi}^2} \sin^2\left(\frac{r}{2}\right) , \quad T_{00}^{(8)} = \frac{1}{2^{10}} \frac{c_8 m^2}{L_r^4 L_{\theta}^4 L_{\phi}^2} \left(8L_{\theta}^2 + (8L_r^2 - L_{\phi}^2) m^2 + 4(L_{\theta}^2 - 2L_r^2 m^2) \cos(r) \right) ,$$

for the $SU(3)$ case.

It is worth to note that the fact that the $N = 3$ solution has lower energy in the ground state than the $N = 2$ solution is an artifact of the model which can be taken into account including subleading corrections in the 't Hooft large- N_c expansion. However, although in the present approach these subleading corrections do not spoil the integrability of the field equations, such corrections certainly make the analytic formulas for the energy density and other relevant physical quantities considerably more cumbersome (see also [34]). Therefore, we decided to consider explicitly only the Skyrme model since it already captures a great deal of novel physical information on the nuclear pasta phase keeping, at the same time, the

analytic formulas readable. We plan to work on the effects of these subleading corrections in a future publication.

4.5 Isospin chemical potential

We have shown in previous sections that the inclusion of a suitable time-dependence in the ansätze, both for lasagna and spaghetti phases (see Eqs. (3.2) and (4.2)), is one of the key ingredients that allows the field equations to be considerably reduced, leading to a single integrable ODE equation for the profiles. This time-dependence offers a nice short-cut to estimate the “classical Isospin” of the configurations analyzed in the present paper (a relevant question is whether or not the classical Isospin is large when the Baryonic charge is large). In particular, one may evaluate the “cost” of removing such time-dependence. Such a cost is related to the internal Isospin symmetry of the theory. This is like trying to estimate the angular momentum of a spinning top by evaluating the cost to make the spinning top to stop spinning. In the present case, the time-dependence of the configurations can be removed from the ansätze by introducing a Isospin chemical potential; then the isospin chemical potential needed to remove such time-dependence is a measure of the classical Isospin of the present configurations. We will see how this works for the simplest $SU(2)$ case, where the generators are $t_j = i\sigma_j$, being σ_j the Pauli matrices (higher $SU(N)$ behave in a similar way).

As it is well known, the effects of the Isospin chemical potential can be taken into account by using the following covariant derivative

$$\nabla_\mu \rightarrow D_\mu = \nabla_\mu + \bar{\mu}[t_3, \cdot]\delta_{\mu 0} . \quad (4.19)$$

Now, we will use exactly the same ansatz as before in the spaghetti $SU(2)$ case, *but this time without the time dependence*:

$$U = e^{\chi(x)(\vec{n} \cdot \vec{t})} , \\ \vec{n} = (\sin \Theta \sin \Phi, \sin \Theta \cos \Phi, \cos \Theta) ,$$

where

$$\chi = \chi(r) , \quad \Theta = q\theta , \quad \Phi = p\phi , \\ q = \frac{1}{2}(2v+1) , \quad p, v \in \mathbb{N} , \quad p \neq 0 ,$$

together with the introduction of the Isospin chemical potential in Eq. (4.19) in the theory. One can check directly that the complete set of Skyrme equations can still be reduced to the same ODE for the profile $\chi(r)$ in the case of the spaghetti phase in Eq. (3.6) *only provided the Isospin chemical potential for the spaghetti phase is given by*

$$\bar{\mu}_S = \frac{p}{L_\phi} . \quad (4.20)$$

In other word, the cost to eliminate the time-dependence is to introduce an Isospin chemical

potential which is large when the Baryonic charge of the spaghetti is large. Something similar happens in the case of the lasagna phase. Let us consider the ansatz in terms of the Euler angles *but without the time-dependence* for the $SU(2)$ case:

$$U_L = e^{\Phi t_3} e^{H t_2} e^{\Theta t_3} ,$$

where

$$\Phi = p\phi , \quad H = h(r) , \quad \Theta = m\theta , \quad p, m \in \mathbb{N} .$$

Let us introduce the Isospin chemical potential, demanding that the profile $h(r)$ should be the same as before. Then, as in the spaghetti case, the Skyrme field equations with chemical potential can still be satisfied by the very same profile $h(r)$ *provided we fix the Isospin chemical potential as*

$$\bar{\mu}_L = \frac{pm}{(p^2 L_\phi^2 + m^2 L_\theta^2)^{\frac{1}{2}}} . \quad (4.21)$$

At this point it is important to remember that in the $SU(2)$ case the lasagna and spaghetti type solutions have the following values for the topological charges

$$B_S = np , \quad B_L = mp ,$$

see [31] and [32] for more details. Therefore, from the above computations it can be seen that the price to pay to eliminate the time-dependence from the configurations discussed in the previous sections is to introduce an Isospin chemical potential which grows as the Baryonic charge of these configurations grows. These arguments show that the “classical Isospin” of configurations with high Baryonic charge is large. Finally, it is important to point out that the large Isospin case corresponds to either neutron rich or proton rich matter and due to Coulomb effects (not taken into account in this model), the neutron rich solution is preferred. This is very nice for the physics relevant for neutron stars⁵.

5 Conclusions and perspectives

In this manuscript, by combining the strategy of [32], [33], [34], [36], [37] and [39] with the generalization of the Euler angles to $SU(N)$ of [42], [43] and [44], we have constructed multi-Baryonic solutions living at finite Baryon density in the $SU(N)$ -Skyrme model for generic values of the number of flavors and with arbitrary values of the topological charge. The energy density of these configurations is concentrated either in tube-shaped regions (suitable to describe the nuclear spaghetti phase) or within Baryonic layers of finite width (suitable to describe the nuclear lasagna phase). To the best of author’s knowledge, this is the first systematic tool to construct analytic topologically non-trivial solutions of such complexity in the $SU(N)$ -Skyrme model for generic N . The physical interest of the present configurations is confirmed, for instance, by the fact that our construction shows explicitly that, at lower densities, configurations with $N = 2$ light flavors are favoured while, at

⁵We thanks the Referee for this valuable comment.

higher densities, configurations with $N = 3$ are favoured. This is a quite non-trivial test of the present approach as a serious analytic candidate to describe the nuclear pasta phase.

The importance of these analytic results arises from the fact that they allow to compare explicitly a relevant physical properties of nuclear lasagna and nuclear spaghetti. For instance, one can see that for high density (but still well within the range of validity of the Skyrme model) the lasagna configurations are favored while at low density the spaghetti configurations are favored. Since the physical properties (such as thermal and electric conductivities) of lasagna and spaghetti phases are very different (see [12] and references therein), our results can have interesting phenomenological implications in high density particles physics, neutron stars and so on. We have also discussed relevant physical quantities (such as the energy per Baryon) which have a smooth large N limit. We hope to come back on the intriguing observable effects related to the present results in a future publication.

Acknowledgments

We are grateful to an anonymous referee, whose comments helped us in severely improve our manuscript.

F. C. has been funded by Fondecyt Grant 1200022. M. L. is funded by FONDECYT post-doctoral Grant 3190873. A. V. is funded by FONDECYT post-doctoral Grant 3200884. The Centro de Estudios Científicos (CECs) is funded by the Chilean Government through the Centers of Excellence Base Financing Program of ANID.

Appendix A: Mathematical tools

In this Appendix we want to recall some main facts about the groups $SU(N)$. Recall that $SU(N)$ is the compact simply connected real group consisting on the set of $N \times N$ complex matrices U satisfying the relations

$$U^\dagger U = \mathbb{I} , \tag{5.1}$$

$$\det U = 1 , \tag{5.2}$$

where \mathbb{I} is the $N \times N$ identity matrix. Its corresponding Lie algebra is the real vector space of traceless anti-Hermitian matrices

$$A = -A^\dagger . \tag{5.3}$$

To see this, consider a curve $U(t) \in SU(N)$, such that $U(0) = \mathbb{I}$. By definition, the element of the Lie algebra are the matrices of the form

$$A = \frac{dU}{dt}(0) .$$

Deriving the relation

$$U(t)^\dagger U(t) = \mathbb{I} ,$$

we get to

$$\frac{dU^\dagger}{dt}(t)U(t) + U(t)^\dagger \frac{dU}{dt}(t) = \mathbb{O} ,$$

where \mathbb{O} is the zero $N \times N$ matrix. Setting $t = 0$ gives $A^\dagger + A = \mathbb{O}$, which show anti-Hermitian-ness. Reality follows from the fact that linear combinations of anti-Hermitian matrices is anti-Hermitian if and only if the coefficients are real. The traceless condition follows from the speciality condition in Eq. (5.2). Indeed, recall that developing the determinant of a matrix X with respect to the j -th row one has

$$\det X = \sum_k x_{jk} \text{cof}_{jk}(X) ,$$

where x_{ij} are the matrix elements and $\text{cof}_{jk}(X)$ is $(-1)^{j+k}$ times the determinant of the reduced matrix after eliminating the j -th row and the k -th column. From this we get to

$$\frac{d}{dx_{jk}} \det X = \text{cof}_{jk}(X) .$$

Therefore, deriving Eq. (5.2) w.r.t. t in $t = 0$ gives (for u_{jk} the matrix elements of U)

$$0 = \frac{d}{dt} \det U \Big|_{t=0} = \sum_{j,k} \frac{d(\det U(t))}{du_{jk}(t)} \frac{du_{jk}}{dt} \Big|_{t=0} = \sum_{j,k} \text{cof}_{jk}(U(0)) A_{jk} . \quad (5.4)$$

On the other hand, using that $U(0) = \mathbb{I}$ and $\text{cof}_{jk}(I) = \delta_{jk}$, we lead to

$$0 = \sum_{j,k} \delta_{jk} A_{jk} = \sum_j A_{jj} = \text{Trace}(A) . \quad (5.5)$$

In particular, $\text{Lie}(SU(N)) \equiv su(N)$ has dimension $(N^2 - 1)$.

Recall that one can back from the algebra to the group by mean of the exponential map

$$\exp : \text{Lie}(G) \longrightarrow G , \quad A \longmapsto \exp A , \quad (5.6)$$

which for a matrix group is

$$\exp A = \mathbb{I} + \sum_{n=1}^{\infty} \frac{1}{n!} A^n .$$

In particular, for a compact Lie group \exp is surjective, so any group element can be written as an exponential. Therefore, fixing a basis t_j for the algebra, any element of the group can be written as

$$g = \exp\left(\sum_j x^j t_j\right) , \quad x^j \in \mathbb{R} .$$

For $SU(N)$ a convenient basis is given by the anti-Hermitian Gell-Mann matrices con-

structed as follows (see [42]):

$$t_{a^2-1} = \sqrt{\frac{2}{a(a-1)}} \left(\sum_{j=1}^{a-1} E_{j,j} - (a-1)E_{a,a} \right), \quad a = 2, \dots, N, \quad (5.7)$$

$$t_1 = -i(E_{1,2} + E_{2,1}), \quad t_2 = E_{1,2} - E_{2,1}, \quad (5.8)$$

$$t_{a^2-1+2j} = E_{j,a+1} - E_{a+1,j}, \quad j = 1, \dots, a, \quad a = 2, \dots, N-1, \quad (5.9)$$

$$t_{a^2-2+2j} = -i(E_{j,a+1} + E_{a+1,j}), \quad j = 1, \dots, a, \quad a = 2, \dots, N-1. \quad (5.10)$$

Here $E_{j,k}$ is the $N \times N$ matrix whose only non zero element is $(E_{j,k})_{jk} = 1$. The Gell-Mann matrices t_A , $A = 1, \dots, (N^2 - 1)$, are normalized, so that

$$-\frac{1}{2} \text{Tr}(t_A t_B) = \delta_{AB}.$$

There are $(N - 1)$ diagonal matrices according to the fact that $SU(N)$ has rank $(N - 1)$. We can also determine the maximal embedding of $SU(2)$ inside $SU(N)$. This is obtained by identifying N as the dimension of an irreducible representation of $SU(2)$. This means that we have to consider the representation of spin $j = (N - 1)/2$. This is standard and given by the matrices in Eqs. (3.3), (3.4) and (3.5). In particular, we see that we get a Bosonic representation for N odd and a Fermionic representation for N even.

Appendix B: Topological charge for the nuclear phases

The allowed values of the topological charge for the spaghetti and lasagna phases depends on the flavor number N , that are explicitly shown in Eqs. (3.11) and (4.6). This determines that for a given value of N the topological charge cannot take arbitrary values. In Table 1, we show the allowed values of the topological charge from $N = 2$ to $N = 10$.

Baryonic charge as $B = B(N)$		
N	<i>Spaghetti</i>	<i>Lasagna</i>
2	$np = \{1, 2, 3, 4, \dots\}$	$m = \{1, 2, 3, 4, \dots\}$
3	$4np = \{4, 8, 12, 16, \dots\}$	$2m = \{2, 4, 6, 8, \dots\}$
4	$10np = \{10, 20, 30, 40, \dots\}$	$10m = \{10, 20, 30, 40, \dots\}$
5	$20np = \{20, 40, 60, 80, \dots\}$	$10m = \{10, 20, 30, 40, \dots\}$
6	$35np = \{35, 70, 105, 140, \dots\}$	$35m = \{35, 70, 105, 140, \dots\}$
7	$56np = \{56, 112, 168, 280, \dots\}$	$28m = \{28, 56, 84, 112, \dots\}$
8	$84np = \{84, 168, 252, 336, \dots\}$	$84m = \{84, 168, 252, 336, \dots\}$
9	$120np = \{120, 240, 360, 480, \dots\}$	$60m = \{60, 120, 180, 240, \dots\}$
10	$165np = \{165, 330, 495, 660, \dots\}$	$165m = \{165, 330, 495, 660, \dots\}$

Table 1: Baryonic charge of the nuclear spaghetti and lasagna phases for different values of N .

References

- [1] D.G. Ravenhall, C.J. Pethick, J.R. Wilson, *Phys. Rev. Lett.* **50**, 2066 (1983).
- [2] M. Hashimoto, H. Seki, M. Yamada, *Prog. Theor. Phys.* **71**, 320 (1984).
- [3] C. J. Horowitz, D. K. Berry, C.M. Briggs, M. E. Caplan, A. Cumming, A. S. Schneider, *Phys. Rev. Lett.* **114**, 031102 (2015).
- [4] D. K. Berry, M. E. Caplan, C. J. Horowitz, G. Huber, A. S. Schneider, *Phys. Rev. C* **94**, 055801 (2016).
- [5] C. O. Dorso, G. A. Frank, J. A. López, *Nucl. Phys. A* **978**, 35 (2018).
- [6] A. da Silva Schneider, M. E. Caplan, D. K. Berry, C. J. Horowitz, *Phys. Rev. C* **98**, 055801 (2018).
- [7] M. E. Caplan, A. S. Schneider, and C. J. Horowitz, *Phys. Rev. Lett.* **121**, 132701 (2018).
- [8] R. Nandi and S. Schramm, *J. Astrophys. Astron.* **39**, 40 (2018).
- [9] Z. Lin, M. E. Caplan, C. J. Horowitz, C. Lunardini, *Phys. Rev. C* **102** (2020) 4, 045801.
- [10] C.O. Dorso, A. Strachan, G.A. Frank, *Nucl. Phys. A* **1002** (2020) 122004.
- [11] C.J. Pethick, Z. Zhang, D.N. Kobyakov, *Phys. Rev. C* **101** (2020) 5, 055802.
- [12] J. A. Lopez, C. O. Dorso, G. A. Frank, *Front. Phys. (Beijing)* **16** (2021) 2, 24301.
- [13] B. Schuetrumpf, G. Martínez-Pinedo, M. Afbuzzaman and H. M. Aktulga, *Phys. Rev. C* **100**, no. 4, 045806 (2019).
- [14] C. C. Barros, D. P. Menezes and F. Gulminelli, *Phys. Rev. C* **101**, no. 3, 035211 (2020).
- [15] J. F. Acevedo, J. Bramante, R. K. Leane and N. Raj, *JCAP* **2003**, 038 (2020).
- [16] Y. Nambu and G. Jona-Lasinio, *Phys. Rev.* **122**, 345 (1961); *Phys. Rev.* **124**, 246 (1961).
- [17] K. Rajagopal and F. Wilczek, in *At the Frontier of Particle Physics/Handbook of QCD*, edited by M. Shifman (World Scientific, Singapore, 2001); arXiv:hep-ph/0011333.
- [18] M. G. Alford, J. A. Bowers, and K. Rajagopal, *Phys. Rev. D* **63**, 074016 (2001).
- [19] R. Casalbuoni and G. Nardulli, *Rev. Mod. Phys.* **76**, 263 (2004).
- [20] T. Skyrme, *Proc. R. Soc. London A* **260**, 127 (1961); *Proc. R. Soc. London A* **262**, 237 (1961); *Nucl. Phys.* **31**, 556 (1962).
- [21] C. G. Callan Jr. and E. Witten, *Nucl. Phys. B* **239** (1984) 161-176.
- [22] E. Witten, *Nucl. Phys.* **B 223** (1983), 422; *Nucl. Phys.* **B 223**, 433 (1983).
- [23] A. P. Balachandran, V. P. Nair, N. Panchapakesan, S. G. Rajeev, *Phys. Rev. D* **28** (1983), 2830.
- [24] A. P. Balachandran, A. Barducci, F. Lizzi, V.G.J. Rodgers, A. Stern, *Phys. Rev. Lett.* **52** (1984), 887; A.P. Balachandran, F. Lizzi, V.G.J. Rodgers, A. Stern, *Nucl. Phys. B* **256**, 525-556 (1985).
- [25] G. S. Adkins, C. R. Nappi, E. Witten, *Nucl. Phys. B* **228** (1983), 552-566.
- [26] N. Manton and P. Sutcliffe, *Topological Solitons*, (Cambridge University Press, Cambridge, 2007).

- [27] A. Balachandran, G. Marmo, B. Skagerstam, A. Stern, *Classical Topology and Quantum States*, World Scientific (1991).
- [28] S. Chen, Y. Li, Y. Yang, *Phys. Rev. D* **89** (2014), 025007.
- [29] F. Canfora, *Phys. Rev. D* **88**, (2013), 065028; E. Ayon-Beato, F. Canfora, J. Zanelli, *Phys. Lett. B* **752**, (2016) 201-205; L. Aviles, F. Canfora, N. Dimakis, D. Hidalgo, *Phys. Rev. D* **96** (2017), 125005; F. Canfora, M. Lagos, S. H. Oh, J. Oliva and A. Vera, *Phys. Rev. D* **98**, no. 8, 085003 (2018); F. Canfora, N. Dimakis, A. Paliathanasis, *Eur.Phys.J. C* **79** (2019) no.2, 139.
- [30] E. Ayon-Beato, F. Canfora, M. Lagos, J. Oliva, A. Vera, *Eur. Phys. J. C* **80**, no. 5, 384 (2020).
- [31] P. D. Alvarez, F. Canfora, N. Dimakis and A. Paliathanasis, *Phys. Lett. B* **773**, (2017) 401-407.
- [32] F. Canfora, *Eur. Phys. J. C* **78**, no. 11, 929 (2018).
- [33] F. Canfora, S.-H. Oh, A. Vera, *Eur.Phys. J. C* **79** (2019) no.6, 485.
- [34] F. Canfora, M. Lagos and A. Vera, *Eur. Phys. J. C* **80**, no. 8, 697 (2020).
- [35] M. Barsanti, S. Bolognesi, F. Canfora, G. Tallarita, *Eur.Phys.J. C* **80** (2020) 12, 1201.
- [36] F. Canfora, S. Carignano, M. Lagos, M. Mannarelli and A. Vera, *Phys. Rev. D* **103**, no. 7, 076003 (2021).
- [37] F. Canfora, A. Giacomini, M. Lagos, S. H. Oh, A. Vera, *Eur.Phys. J. C* **81** (2021) 1, 55.
- [38] F. Canfora, A. Cisterna, D. Hidalgo and J. Oliva, *Phys. Rev. D* **103**, no. 8, 085007 (2021).
- [39] P. D. Alvarez, S. L. Cacciatori, F. Canfora and B. L. Cerchiai, *Phys. Rev. D* **101**, no. 12, 125011 (2020).
- [40] A. Jackson, *Nucl. Phys. A* **493**, 365-383 (1989); *Nucl. Phys. A* **496**, 667 (1989).
- [41] M. Nitta, N. Shiiki, *Prog. Theor. Phys.* 119, 829-838 (2008).
- [42] S. Bertini, S. L. Cacciatori, B. L. Cerchiai, *J. Math. Phys. (N.Y.)* 47, 043510 (2006).
- [43] S. L. Cacciatori, F. Dalla Piazza, and A. Scotti, *Trans. Am. Math. Soc.* 369, 4709 (2017).
- [44] T. E. Tilma and G. Sudarshan, *J. Geom. Phys.* 52, 263 (2004).
- [45] Newton, W. G., *Nature Physics*, vol. 9, 396-397 (2013).
- [46] Pons, J. A., Vigano, D. & Rea, N. *Nature Phys.* 9, 431-434 (2013).
- [47] G. S. Adkins and C. R. Nappi, *Phys. Lett. B* **137**, 251-256 (1984).
- [48] L. Marleau, *Phys. Lett. B* 235, 141 (1990); Erratum: [*Phys. Lett. B* 244, 580 (1990)]; *Phys. Rev. D* 43, 885 (1991); *Phys. Rev. D* 45, 1776 (1992).
- [49] A. Jackson, A. Jackson, A. Goldhaber, G. Brown and L. Castillejo, *Phys. Lett. B* **154**, 101-106 (1985).
- [50] G.S. Adkins, C.R. Nappi, *Phys. Lett. B* 137, 251-256 (1984).
- [51] S. B. Gudnason, M. Nitta, *JHEP* **1709**, 028 (2017).
- [52] Al-Zamel, A., Tuan, V.K., Kalla, S.L. , *Appl. Math. Comput.*, 114 (2000), 13 25; Garg, Mridula, Katta, Vimal, and Kalla, S. , *Serdica Mathematical Journal* 27.3 (2001): 219-232; Garg, M., Katta, V., Kalla, S.L. , *Appl. Math. Comput.*, 131 (2002), 607 613.

- [53] M. Shifman, “*Advanced Topics in Quantum Field Theory: A Lecture Course*” Cambridge University Press, (2012).
- [54] M. Shifman, A. Yung, “*Supersymmetric Solitons*” Cambridge University Press, (2009).
- [55] G. 't Hooft, Nucl. Phys. B 72, 461 (1974); Nucl. Phys. B 75, 461 (1974).
- [56] G. Veneziano, Nucl. Phys. B117, 519 (1976).
- [57] E. Witten, Nucl. Phys. B 160, 57 (1979).
- [58] S. Scherer, Adv. Nucl. Phys. **27**, 277 (2003).
- [59] E. B. Dynkin, “Semisimple subalgebras of semisimple Lie algebras,” Am. Math. Soc. Transl., Ser. 2 6, 111, 245 (1957).